Fundamental implicit FDTD schemes for computational electromagnetics and educational mobile apps

Tan, Eng Leong

2020

Tan, E. L. (2020). Fundamental implicit FDTD schemes for computational electromagnetics and educational mobile apps. Progress In Electromagnetics Research, 168, 39-59. https://dx.doi.org/10.2528/PIER20061002

https://hdl.handle.net/10356/149186

https://doi.org/10.2528/PIER20061002

Progress In Electromagnetics Research, Vol. 168, 39–59, 2020

Fundamental Implicit FDTD Schemes for Computational Electromagnetics and Educational Mobile APPS

Eng Leong Tan*

(*Invited Review*)

Abstract—This paper presents an overview and review of the fundamental implicit finite-difference time-domain (FDTD) schemes for computational electromagnetics (CEM) and educational mobile apps. The fundamental implicit FDTD schemes are unconditionally stable and feature the most concise update procedures with matrix-operator-free right-hand sides (RHS). We review the developments of fundamental implicit schemes, which are simpler and more efficient than all previous implicit schemes having RHS matrix operators. They constitute the basis of unification for many implicit schemes including classical ones, providing insights into their inter-relations along with simplifications, concise updates and efficient implementations. Based on the fundamental implicit schemes, further developments can be carried out more conveniently. Being the core CEM on mobile apps, the multiple one-dimensional (M1-D) FDTD methods are also reviewed. To simulate multiple transmission lines, stubs and coupled transmission lines efficiently, the M1-D explicit FDTD method as well as the unconditionally stable M1-D fundamental alternating direction implicit (FADI) FDTD and coupled line (CL) FDTD methods are discussed. With the unconditional stability of FADI methods, the simulations are fast-forwardable with enhanced efficiency. This is very useful for quick concept illustrations or phenomena demonstrations during interactive teaching and learning. Besides time domain, many frequency-domain methods are well-suited for further developments of useful mobile apps as well.

1. INTRODUCTION

Computational electromagnetics (CEM) are a key to the design and analysis of modern antennas, waveguides, wireless communication systems, etc. One of the most popular CEM methods in time domain is finite-difference time-domain (FDTD) method [1, 2]. However, the conventional FDTD method is an explicit scheme and becomes unstable when the time step size is larger than Courant-Friedrichs-Lewy (CFL) stability constraint. To overcome the CFL constraint, unconditionally stable alternating direction implicit (ADI) FDTD method has been developed [3, 4]. Such unconditional stability comes at the expense of being complicated and inefficient in its implementations. This is because there are not only matrix operators at the left-hand-sides (LHS) making it implicit scheme, even the right-hand-sides (RHS) of update procedures also comprise matrix operators that call for considerable floating-point operations (flops). This has motivated alternative implicit FDTD schemes in an attempt to improve the simplicity and efficiency.

Over the years, we have introduced and developed several unconditionally stable implicit FDTD schemes, including split-step (SS) FDTD and locally one-dimensional (LOD) FDTD methods, etc., [5–7]. In particular, the LOD-FDTD method is for '3-D' Maxwell's equations, second-order temporal-accurate and more efficient than ADI-FDTD. Still, these alternative implicit FDTD schemes remain

Received 10 June 2020, Accepted 12 September 2020, Scheduled 3 October 2020

* Corresponding author: Eng Leong Tan (eeltan@ntu.edu.sg).

The author is with the School of Electrical and Electronic Engineering, Nanyang Technological University, 639798, Singapore. This is an Electromagnetics Academy Fellow Elevation Journal Article (on the author's research works related to CEM and mobile apps).

complicated with a variety of matrix operators at their RHS. In our continued efforts to further improve the simplicity and efficiency, we have introduced the fundamental implicit FDTD schemes [8], which are unconditionally stable and feature the most concise update procedures with matrix-operator-free RHS. This paper reviews the developments of fundamental implicit schemes, which are simpler and more efficient than all previous implicit schemes having RHS matrix operators. They constitute the basis of unification for many implicit schemes including classical ones, providing insights into their inter-relations along with simplifications, concise updates and efficient implementations. The classical schemes as well as ADI-, SS- and LOD-FDTD methods with two or three split matrices, etc., can all be simplified into concise and efficient forms with matrix-operator-free RHS, cf. Section 2. Based on the fundamental implicit schemes, further developments can be carried out more conveniently, and they may also be extended readily to other branches of physics.

Meanwhile, most CEM involving full-wave 3-D computations like above often call for large computing resources and are typically not suitable for mobile devices. To enable real-time electromagnetic (EM) simulations on mobile devices, there is a need for innovative CEM that are well-suited for their efficient implementations. We have developed several educational mobile apps, e.g., *MuStripKit, EMpolarization, EMwaveRT*, etc. (some on App/Play Store) [9–14], which are incorporated with innovative CEM that could run efficiently on mobile devices (smartphones/ipads, supplementable with 3-D displays). Exploiting the wide affordances of mobile devices, these mobile apps are useful for quick initial design, analysis and seamless teaching/learning anytime, anywhere. They provide touch-based interactivity and real-time EM+circuit simulations, as well as 2-D/3-D visualizations of wave phenomena to enhance teaching and learning of electromagnetics. Being the core CEM on mobile apps, we also review in this paper the multiple one-dimensional (M1-D) FDTD methods that bypass the computationally intensive 3-D ones. To simulate multiple transmission lines, stubs and coupled transmission lines efficiently, the (conditionally stable) M1-D explicit FDTD method as well as the unconditionally stable M1-D fundamental alternating direction implicit (FADI) FDTD and coupled line (CL)-FDTD methods are discussed, cf. Section 3. Besides time domain, many frequency-domain methods are well-suited for further developments of useful mobile apps as well. They can be extended further for advanced analyses in electromagnetics and beyond.

2. FUNDAMENTAL IMPLICIT FDTD SCHEMES FOR COMPUTATIONAL ELECTROMAGNETICS

2.1. Fundamental Implicit Schemes for ADI-FDTD Method and Classical Schemes

The 3-D Maxwell's curl equations can be written in compact matrix form

$$\frac{\partial \mathbf{u}}{\partial t} = \mathbf{W}\mathbf{u}, \quad \mathbf{W} = \mathbf{A} + \mathbf{B} \tag{1a}$$

$$\mathbf{u} = [E_x \quad E_y \quad E_z \quad H_x \quad H_y \quad H_z]^T \tag{1b}$$

where $\mathbf{u}$ is the EM field vector; $\mathbf{W}$ is the 6×6 Maxwell system matrix; $\mathbf{A}$ and $\mathbf{B}$ are its two split matrix operators. Equations (1a)–(1b) can be solved using the explicit FDTD scheme with leapfrog time-stepping on staggered Yee's grids, with the time step size subjected to the CFL stability constraint $\Delta t \leq \Delta t_{\text{CFL}}$ [1, 2]. To overcome such stability constraint, unconditionally stable ADI-FDTD method has been introduced with two update procedures as [3, 4]

$$\left(\mathbf{I} - \frac{\Delta t}{2}\mathbf{A}\right)\mathbf{u}^{n+\frac{1}{2}} = \left(\mathbf{I} + \frac{\Delta t}{2}\mathbf{B}\right)\mathbf{u}^{n} \tag{2a}$$

$$\left(\mathbf{I} - \frac{\Delta t}{2}\mathbf{B}\right)\mathbf{u}^{n+1} = \left(\mathbf{I} + \frac{\Delta t}{2}\mathbf{A}\right)\mathbf{u}^{n+\frac{1}{2}}. \tag{2b}$$

Here and henceforth, $\mathbf{I}$ is the identity matrix, and $\mathbf{u}$'s with integers in the superscripts, e.g., $\mathbf{u}^n$ and $\mathbf{u}^{n+1}$, denote the main field vectors with second-order temporal accuracy (unless otherwise specified via the subscripts). All other intermediate or auxiliary field vectors, e.g., $\mathbf{u}^{n+\frac{1}{2}}$ and subsequent $\mathbf{u}^*$, $\mathbf{v}$'s, etc., are typically of lower order and would not be of much interest usually. The split matrix operators

A and **B** are given specifically by

$$\mathbf{A} = \begin{bmatrix} 0 & 0 & 0 & 0 & 0 & \frac{1}{\epsilon}\frac{\partial}{\partial y} \\ 0 & 0 & 0 & \frac{1}{\epsilon}\frac{\partial}{\partial z} & 0 & 0 \\ 0 & 0 & 0 & 0 & \frac{1}{\epsilon}\frac{\partial}{\partial x} & 0 \\ 0 & \frac{1}{\mu}\frac{\partial}{\partial z} & 0 & 0 & 0 & 0 \\ 0 & 0 & \frac{1}{\mu}\frac{\partial}{\partial x} & 0 & 0 & 0 \\ \frac{1}{\mu}\frac{\partial}{\partial y} & 0 & 0 & 0 & 0 & 0 \end{bmatrix} \tag{3a}$$

$$\mathbf{B} = \begin{bmatrix} 0 & 0 & 0 & 0 & \frac{-1}{\epsilon}\frac{\partial}{\partial z} & 0 \\ 0 & 0 & 0 & 0 & 0 & \frac{-1}{\epsilon}\frac{\partial}{\partial x} \\ 0 & 0 & 0 & \frac{-1}{\epsilon}\frac{\partial}{\partial y} & 0 & 0 \\ 0 & 0 & \frac{-1}{\mu}\frac{\partial}{\partial y} & 0 & 0 & 0 \\ \frac{-1}{\mu}\frac{\partial}{\partial z} & 0 & 0 & 0 & 0 & 0 \\ 0 & \frac{-1}{\mu}\frac{\partial}{\partial x} & 0 & 0 & 0 & 0 \end{bmatrix}. \tag{3b}$$

Equations (2a)–(2b) represent the generalized formulae of classical ADI scheme [15–17]. While gaining improved stability, such an implicit scheme involves matrix operators at the LHS of update procedures, which necessitate certain matrix inversions making the solution process 'implicit'. Moreover, the RHS of update procedures also comprise matrix operators, which call for considerable flops count leading to reduced efficiency for each update. This is unlike the explicit scheme that is conditionally stable but does not involve any LHS matrix operator, thus bypassing the inversion of matrix and making the solution process 'explicit'. Due to the unconditional stability of ADI-FDTD, one may exploit the use of time step size larger than the CFL constraint.

To improve the efficiency, we introduce the auxiliary field vectors **v**'s along with the following update procedures [8, 18]:

$$\mathbf{v}^n = \mathbf{u}^n - \mathbf{v}^{n-\frac{1}{2}} \tag{4a}$$

$$\left(\frac{1}{2}\mathbf{I} - \frac{\Delta t}{4}\mathbf{A}\right)\mathbf{u}^{n+\frac{1}{2}} = \mathbf{v}^n \tag{4b}$$

$$\mathbf{v}^{n+\frac{1}{2}} = \mathbf{u}^{n+\frac{1}{2}} - \mathbf{v}^n \tag{4c}$$

$$\left(\frac{1}{2}\mathbf{I} - \frac{\Delta t}{4}\mathbf{B}\right)\mathbf{u}^{n+1} = \mathbf{v}^{n+\frac{1}{2}}. \tag{4d}$$

Unlike the previous ADI scheme in Eqs. (2a)–(2b), the RHS of Eqs. (4a)–(4d) contain only vectors and are matrix-operator-free (no more **A** or **B**), while their LHS involve similar matrix operators (to within a factor $\frac{1}{2}$). Based on the 'fundamental' adjective which means basic and not able to be divided or reduced any further (according to dictionaries, e.g., Oxford), this scheme is aptly called fundamental ADI-FDTD, or in short, FADI scheme. Such a fundamental scheme is indeed not reducible any further because there is no more matrix operator to be omitted at the RHS of implicit scheme (recall that the LHS matrix operator cannot be simply omitted because the scheme should stay 'implicit' and stable.) Note that although there are additional **v** variables, there is no need for extra memory array because they are only temporary and reusable. The advantages of FADI scheme include concise update procedures with matrix-operator-free RHS, which result in simple, convenient coding and efficient implementation. This would also lead to simple, concise and efficient incorporation of current sources [19]. If there exist non-zero initial fields $\mathbf{u}^0$, one can perform the following input processing that is required only once at the initial step $n = 0$:

$$\text{Input:} \quad \mathbf{v}^{-\frac{1}{2}} = \left(\frac{1}{2}\mathbf{I} - \frac{\Delta t}{4}\mathbf{B}\right)\mathbf{u}^0. \tag{5}$$

The fundamental implicit scheme above exploits the auxiliary field vectors to omit as many RHS matrix operators as possible, especially when there are similar ones present at the LHS of update

procedures. Applying the same principle of fundamental implicit scheme, many other classical implicit schemes besides ADI can be transformed to the same form involving update procedures with matrix-operator-free RHS. These classical implicit schemes are discussed below in their generalized formulae representations.

- Douglas scheme [20] or Crank-Nicolson direct-splitting (CNDS) method [21, 22]:

$$\left(\mathbf{I}-\frac{\Delta t}{2}\mathbf{A}\right)\mathbf{u}^{*}_{\mathrm{DS}} = \left(\mathbf{I}+\frac{\Delta t}{2}\mathbf{A}+\Delta t\mathbf{B}\right)\mathbf{u}^{n} \tag{6a}$$

$$\left(\mathbf{I}-\frac{\Delta t}{2}\mathbf{B}\right)\mathbf{u}^{n+1} = \mathbf{u}^{*}_{\mathrm{DS}}-\frac{\Delta t}{2}\mathbf{B}\mathbf{u}^{n}. \tag{6b}$$

  The corresponding fundamental implicit scheme is the same as above, i.e.,

$$\text{(6a)–(6b)} \iff \text{(4a)–(4d)} \quad \text{via} \quad \mathbf{u}^{*}_{\mathrm{DS}} = 2\mathbf{u}^{n+\frac{1}{2}}-\mathbf{u}^{n}. \tag{7}$$

- Douglas-Gunn scheme or delta formulation [17, (5.8.37)–(5.8.38)]:

$$\left(\mathbf{I}-\frac{\Delta t}{2}\mathbf{A}\right)\Delta\mathbf{u}^{*} = \Delta t\left(\mathbf{A}+\mathbf{B}\right)\mathbf{u}^{n} \tag{8a}$$

$$\left(\mathbf{I}-\frac{\Delta t}{2}\mathbf{B}\right)\Delta\mathbf{u} = \Delta\mathbf{u}^{*} \tag{8b}$$

$$\mathbf{u}^{n+1} = \mathbf{u}^{n}+\Delta\mathbf{u}. \tag{8c}$$

  The corresponding fundamental implicit scheme is the same as above, i.e.,

$$\text{(8a)–(8c)} \iff \text{(4a)–(4d)} \quad \text{via} \quad \Delta\mathbf{u}^{*} = 2\left(\mathbf{u}^{n+\frac{1}{2}}-\mathbf{u}^{n}\right). \tag{9}$$

- D'Yakonov scheme [17, (4.4.14)–(4.4.15)], Beam-Warming scheme [17, (5.8.34)–(5.8.35)], or Crank-Nicolson Douglas-Gunn (CNDG) method [21]:

$$\left(\mathbf{I}-\frac{\Delta t}{2}\mathbf{A}\right)\mathbf{u}^{*}_{\mathrm{DY}} = \left(\mathbf{I}+\frac{\Delta t}{2}\mathbf{A}\right)\left(\mathbf{I}+\frac{\Delta t}{2}\mathbf{B}\right)\mathbf{u}^{n} \tag{10a}$$

$$\left(\mathbf{I}-\frac{\Delta t}{2}\mathbf{B}\right)\mathbf{u}^{n+1} = \mathbf{u}^{*}_{\mathrm{DY}}. \tag{10b}$$

  The corresponding fundamental implicit scheme is the same as above, i.e.,

$$\text{(10a)–(10b)} \iff \text{(4a)–(4d)} \quad \text{via} \quad \mathbf{u}^{*}_{\mathrm{DY}} = 2\mathbf{v}^{n+\frac{1}{2}}. \tag{11}$$

The above classical implicit schemes call for update procedures with various RHS involving sum [cf. Eqs. (6a), (8a)] and/or product [cf. Eq. (10a)] of matrix operators. Equations (4a)–(4d) provide their simplifications into concise and efficient forms with matrix-operator-free RHS (no more **A** or **B**). Table 1 lists the flops count for RHS of update equations in one full time step for implicit FDTD schemes. The flops count includes addition/subtraction ($+$ or $-$), multiplication/division ($\times$ or $\div$) and total operations at the RHS of update equations, with the same number of operations for the LHS (~ 30 flops). From

Table 1. Flops count for RHS of update equations in one full time step for implicit FDTD schemes.

Implicit FDTD Scheme	Equations	$+$ or $-$	$\times$ or $\div$	Total
ADI	(2a)–(2b)	72	36	108
Douglas/CNDS	(6a)–(6b)	90	36	126
Douglas-Gunn/delta	(8a)–(8c)	66	33	99
D'Yakonov/Beam-Warming/CNDG	(10a)–(10b)	102	48	150
Fundamental	(4a)–(4d)	30	12	42

the table, one can see clearly that the total flops count for ADI and each classical implicit scheme has been reduced significantly, i.e., from $\sim$ 100–150 flops to merely 42 flops in the fundamental implicit scheme. Moreover, it is not obvious at first glance how the classical implicit schemes in their original formulae are related to each other and the ADI scheme. By using the respective auxiliary field relations in their fundamental implicit schemes with similar forms, one can show the equivalence among them readily as in Eqs. (7), (9) and (11). Therefore, the fundamental implicit schemes constitute the basis of unification for many implicit schemes, providing insights into their inter-relations (or equivalence) along with simplifications, concise updates and efficient implementations.

Based on the fundamental implicit schemes, further developments can be carried out more conveniently for ADI and classical schemes. The developments may include higher order spatial accuracy [23], compact [24] and parameter optimized [25] methods, lossy [26–32], dispersive [33–41] and biological media [42, 43], lumped networks and elements [44–48], implicit update for magnetic fields [49], absorbing boundary conditions [50, 51], total-field/scattered-field formulations [52–54], complex-envelope methods for anisotropic photonic crystals [55, 56], etc.

2.2. Fundamental Implicit Schemes for SS- and LOD-FDTD Methods

Alternative to the ADI-FDTD method above, unconditionally stable SS- and LOD-FDTD methods have also been developed with the same two split matrix operators as [5–7]

$$\left(\mathbf{I}-\frac{\Delta t}{2}\mathbf{A}\right)\mathbf{u}^{n+\frac{1}{2}} = \left(\mathbf{I}+\frac{\Delta t}{2}\mathbf{A}\right)\mathbf{u}_1^{n} \tag{12a}$$

$$\left(\mathbf{I}-\frac{\Delta t}{2}\mathbf{B}\right)\mathbf{u}_1^{n+1} = \left(\mathbf{I}+\frac{\Delta t}{2}\mathbf{B}\right)\mathbf{u}^{n+\frac{1}{2}}. \tag{12b}$$

Equations (12a)–(12b) represent the generalized formulae of classical LOD scheme with two update procedures [57]. Their RHS still involve the matrix operators like (2a)–(2b), which are now the same as those of LHS for each update, i.e., $\mathbf{A}$ in the LHS and RHS of (12a), $\mathbf{B}$ in the LHS and RHS of (12b), respectively. Due to the non-commutativity of matrix operators, this scheme is only accurate to first order in time and may be denoted by SS1 or LOD1. To signify such first-order temporal accuracy, the main field vectors with integers in the superscripts are subscripted as $\mathbf{u}_1$, to distinguish from the unsubscripted (second-order temporal-accurate) $\mathbf{u}$ above. (The accuracy orders of other intermediate or auxiliary field vectors are not of much interest and their variables would not be subscripted.)

To improve the efficiency, we apply the principle of fundamental implicit schemes and introduce the auxiliary field vectors in the update procedures as [8, 58]

$$\left(\frac{1}{2}\mathbf{I}-\frac{\Delta t}{4}\mathbf{A}\right)\mathbf{v}^{n+\frac{1}{2}} = \mathbf{u}_1^{n} \tag{13a}$$

$$\mathbf{u}^{n+\frac{1}{2}} = \mathbf{v}^{n+\frac{1}{2}} - \mathbf{u}_1^{n} \tag{13b}$$

$$\left(\frac{1}{2}\mathbf{I}-\frac{\Delta t}{4}\mathbf{B}\right)\mathbf{v}^{n+1} = \mathbf{u}^{n+\frac{1}{2}} \tag{13c}$$

$$\mathbf{u}_1^{n+1} = \mathbf{v}^{n+1} - \mathbf{u}^{n+\frac{1}{2}}. \tag{13d}$$

In these procedures, all their RHS have been simplified in concise and efficient matrix-operator-free forms (no more $\mathbf{A}$ or $\mathbf{B}$). This scheme can be aptly called fundamental LOD-FDTD, or in short, FLOD scheme, while FLOD1 or FSS1 may also be referred occasionally to signify its first-order temporal accuracy. Despite sharing the same notations, the $\mathbf{v}$'s of FLOD are different from those of FADI. In fact, by comparing Eq. (13d) (at one time step backward, $n+1 \to n$) and Eqs. (13a)–(13c) of FLOD with Eqs. (4a)–(4d) of FADI, one can readily find that their $\mathbf{u}$'s and $\mathbf{v}$'s are simply interchanged between both schemes. This also explains the first-order temporal accuracy of $\mathbf{u}_1$ from the output of Eq. (13d), which is merely like the auxiliary field vector $\mathbf{v}$ in Eq. (4a). From here, we see again that the fundamental implicit schemes constitute the basis of unification for ADI and SS1/LOD1 schemes, providing insights into their inter-relations along with simplifications, concise updates and efficient implementations [59].

The FLOD1 scheme is useful especially when high accuracy is not needed, such as during initial design, analysis, teaching and learning, etc. To recover the usual second-order temporal accuracy, we

resort to the update procedures in Eqs. (13a)–(13d) as they are, along with the following input and output processings [7]:

$$\text{Input:} \quad \left(\frac{1}{2}\mathbf{I}-\frac{\Delta t}{8}\mathbf{B}\right)\mathbf{v}_*^0=\mathbf{u}_{\text{LOD2}}^0, \quad \mathbf{u}_1^0=\mathbf{v}_*^0-\mathbf{u}_{\text{LOD2}}^0 \tag{14a}$$

$$\text{Output:} \quad \left(\frac{1}{2}\mathbf{I}+\frac{\Delta t}{8}\mathbf{B}\right)\mathbf{v}_*^{n+1}=\mathbf{u}_1^{n+1}, \quad \mathbf{u}_{\text{LOD2}}^{n+1}=\mathbf{v}_*^{n+1}-\mathbf{u}_1^{n+1}. \tag{14b}$$

The input processing in Eq. (14a) is required only once at the initial step if there exist non-zero initial fields $\mathbf{u}_{\text{LOD2}}^0$, which should be second-order temporal-accurate. The output processing in Eq. (14b) is to be performed independently of the main iterations, only when the output data $\mathbf{u}_{\text{LOD2}}^{n+1}$ is needed. Furthermore, it may be executed only for the required field components at some specific observation points or planes. Exploiting the careful treatments via proper input and infrequent output processings for Eqs. (13a)–(13d), one can achieve second-order temporal accuracy (as signified by '2') in $\mathbf{u}_{\text{LOD2}}^{n+1}$ for FLOD2 scheme, along with overall high efficiency comparable to FADI.

While the above treatments involve mostly implicit solutions, we also consider other input and output processings as [60–62]

$$\text{Input:} \quad \left(\mathbf{I}-\frac{\Delta t}{2}\mathbf{B}\right)\mathbf{u}_1^0=\mathbf{u}_{\text{CD2}}^0 \tag{15a}$$

$$\text{Output:} \quad \mathbf{u}_{\text{CD2}}^{n+1}=\left(\mathbf{I}-\frac{\Delta t}{2}\mathbf{B}\right)\mathbf{u}_1^{n+1}. \tag{15b}$$

In conjunction with the update procedures in Eqs. (13a)–(13d), Eqs. (15a)–(15b) lead to not only second-order temporal accuracy, but also complying divergence (as signified by 'CD') in the output $\mathbf{u}_{\text{CD2}}^{n+1}$. This scheme can thus be aptly called fundamental LOD2-CD-FDTD, or in short, FLOD2-CD scheme. Moreover, the output processing in Eq. (15b) is performed in an explicit manner independently of the main iterations, only when the output data is needed for the required particular field components at some specific observation locations.

The original classical SS scheme may also achieve second-order temporal accuracy with three update procedures given by [5, 6]

$$\left(\mathbf{I}-\frac{\Delta t}{4}\mathbf{A}\right)\mathbf{u}^{n+\frac{1}{4}}=\left(\mathbf{I}+\frac{\Delta t}{4}\mathbf{A}\right)\mathbf{u}_{\text{SS2}}^{n} \tag{16a}$$

$$\left(\mathbf{I}-\frac{\Delta t}{2}\mathbf{B}\right)\mathbf{u}^{n+\frac{3}{4}}=\left(\mathbf{I}+\frac{\Delta t}{2}\mathbf{B}\right)\mathbf{u}^{n+\frac{1}{4}} \tag{16b}$$

$$\left(\mathbf{I}-\frac{\Delta t}{4}\mathbf{A}\right)\mathbf{u}_{\text{SS2}}^{n+1}=\left(\mathbf{I}+\frac{\Delta t}{4}\mathbf{A}\right)\mathbf{u}^{n+\frac{3}{4}}. \tag{16c}$$

As before, applying the principle of fundamental implicit schemes leads to the fundamental SS2-FDTD or FSS2 scheme [63]:

$$\left(\frac{1}{2}\mathbf{I}-\frac{\Delta t}{8}\mathbf{A}\right)\mathbf{v}^{n+\frac{1}{4}}=\mathbf{u}_{\text{SS2}}^{n}, \quad \mathbf{u}^{n+\frac{1}{4}}=\mathbf{v}^{n+\frac{1}{4}}-\mathbf{u}_{\text{SS2}}^{n} \tag{17a}$$

$$\left(\frac{1}{2}\mathbf{I}-\frac{\Delta t}{4}\mathbf{B}\right)\mathbf{v}^{n+\frac{3}{4}}=\mathbf{u}^{n+\frac{1}{4}}, \quad \mathbf{u}^{n+\frac{3}{4}}=\mathbf{v}^{n+\frac{3}{4}}-\mathbf{u}^{n+\frac{1}{4}} \tag{17b}$$

$$\left(\frac{1}{2}\mathbf{I}-\frac{\Delta t}{8}\mathbf{A}\right)\mathbf{v}^{n+1}=\mathbf{u}^{n+\frac{3}{4}}, \quad \mathbf{u}_{\text{SS2}}^{n+1}=\mathbf{v}^{n+1}-\mathbf{u}^{n+\frac{3}{4}}. \tag{17c}$$

To further increase the accuracy order in time, we have developed the SS4-FDTD method with fourth order temporal accuracy, which requires nine update procedures with a systematic sequence of time-stepping coefficients [64]. Another method with fourth order temporal accuracy has also been derived based on ADI-FDTD that requires six update procedures [65]. All these higher order methods may be simplified into their fundamental implicit schemes, which feature concise and efficient matrix-operator-free RHS in the multi-stage update procedures. Note that the multi-stage SS and

ADI methods along with their temporal orders of accuracy can be interpreted based on the matrix exponential [66], which represents the exact solution to Maxwell's differential equations. Such matrix exponential interpretation is more general than the traditional Crank-Nicolson perturbation and is useful to ascertain the correct temporal order for ADI [67] and other multi-stage implicit schemes [68]. Using the matrix exponential interpretation also allows one to deduce new schemes, e.g., one that is second-order accurate and divergence-preserving.

Further developments of the above SS-, LOD- and ADI-FDTD methods can be carried out conveniently based on their fundamental implicit schemes. The developments may include further acceleration on graphics processor units (GPU) [69, 70], inclusion of absorbing, PMC and PEC boundary conditions [71, 72], total-field/scattered-field techniques [73], extension to general anisotropic media [74], complex-envelope method [75], lumped elements [76, 77], memristor [78, 79], etc. Note that the LOD-FDTD method remains stable even for non-uniform (varying) time-steps during run-time [80]. Other implicit FDTD methods (e.g., ADI-FDTD) tend to become unstable unless the time step is uniform throughout [81]. Besides electromagnetics, all the methods based on fundamental implicit schemes may also be extended readily to other branches of physics such as thermodynamics [82–86] and quantum mechanics [87], etc.

2.3. Fundamental Implicit Scheme for Leapfrog ADI-FDTD Method

The leapfrog ADI-FDTD method involves time-staggered fields with update procedures as [88]

$$\left(\mathbf{I}-\frac{\Delta t^2}{4}\mathbf{A}_{12}\mathbf{A}_{21}\right)\mathbf{E}^{n+\frac{1}{2}} = \left(\mathbf{I}-\frac{\Delta t^2}{4}\mathbf{A}_{12}\mathbf{A}_{21}\right)\mathbf{E}^{n-\frac{1}{2}} + \Delta t\left(\mathbf{A}_{12}+\mathbf{B}_{12}\right)\mathbf{H}^{n} \tag{18a}$$

$$\left(\mathbf{I}-\frac{\Delta t^2}{4}\mathbf{B}_{21}\mathbf{B}_{12}\right)\mathbf{H}^{n+1} = \left(\mathbf{I}-\frac{\Delta t^2}{4}\mathbf{B}_{21}\mathbf{B}_{12}\right)\mathbf{H}^{n} + \Delta t\left(\mathbf{A}_{21}+\mathbf{B}_{21}\right)\mathbf{E}^{n+\frac{1}{2}} \tag{18b}$$

where $\mathbf{A}_{ij}$ and $\mathbf{B}_{ij}$ are the 3×3 submatrices of $\mathbf{A}$ and $\mathbf{B}$:

$$\mathbf{A}_{12} = \begin{bmatrix} 0 & 0 & \frac{1}{\epsilon}\frac{\partial}{\partial y} \\ \frac{1}{\epsilon}\frac{\partial}{\partial z} & 0 & 0 \\ 0 & \frac{1}{\epsilon}\frac{\partial}{\partial x} & 0 \end{bmatrix}, \quad \mathbf{A}_{21} = \begin{bmatrix} 0 & \frac{1}{\mu}\frac{\partial}{\partial z} & 0 \\ 0 & 0 & \frac{1}{\mu}\frac{\partial}{\partial x} \\ \frac{1}{\mu}\frac{\partial}{\partial y} & 0 & 0 \end{bmatrix} \tag{19a}$$

$$\mathbf{B}_{12} = \begin{bmatrix} 0 & \frac{-1}{\epsilon}\frac{\partial}{\partial z} & 0 \\ 0 & 0 & \frac{-1}{\epsilon}\frac{\partial}{\partial x} \\ \frac{-1}{\epsilon}\frac{\partial}{\partial y} & 0 & 0 \end{bmatrix}, \quad \mathbf{B}_{21} = \begin{bmatrix} 0 & 0 & \frac{-1}{\mu}\frac{\partial}{\partial y} \\ \frac{-1}{\mu}\frac{\partial}{\partial z} & 0 & 0 \\ 0 & \frac{-1}{\mu}\frac{\partial}{\partial x} & 0 \end{bmatrix}. \tag{19b}$$

Notice that the RHS of Eqs. (18a)–(18b) involve considerable matrix operators including second-order ones.

To improve the efficiency, we could make use of the principle of fundamental implicit schemes to omit as many RHS matrix operators as possible, especially when there are similar ones present at the LHS. Introducing the auxiliary variables $\mathbf{e}$ and $\mathbf{h}$, the update procedures can be written as

$$\left(\mathbf{I}-\frac{\Delta t^2}{4}\mathbf{A}_{12}\mathbf{A}_{21}\right)\mathbf{e}^{n+\frac{1}{2}} = \Delta t\left(\mathbf{A}_{12}+\mathbf{B}_{12}\right)\mathbf{H}^{n} \tag{20a}$$

$$\mathbf{E}^{n+\frac{1}{2}} = \mathbf{e}^{n+\frac{1}{2}} + \mathbf{E}^{n-\frac{1}{2}} \tag{20b}$$

$$\left(\mathbf{I}-\frac{\Delta t^2}{4}\mathbf{B}_{21}\mathbf{B}_{12}\right)\mathbf{h}^{n+1} = \Delta t\left(\mathbf{A}_{21}+\mathbf{B}_{21}\right)\mathbf{E}^{n+\frac{1}{2}} \tag{20c}$$

$$\mathbf{H}^{n+1} = \mathbf{h}^{n+1} + \mathbf{H}^{n}. \tag{20d}$$

Compared to Eqs. (18a)–(18b), the RHS of Eqs. (20a)–(20d) no longer involve the second-order matrix operators. This makes the update procedures more concise and efficient, which may be regarded as the fundamental leapfrog ADI-FDTD method.

Further analyses of the leapfrog ADI-FDTD method have been carried out including stability, dispersion [89] and divergence properties [90, 91]. The method has also been extended to lossy media [92]

and non-penetrable targets [93]. For the latter, there are nonphysical field leakage problems, which can be resolved with infinite permittivity approach. Note that the leapfrog ADI-FDTD method does not have complying divergence and exhibits non-zero divergence in source-free regions. This can be overcome by using the FLOD2-CD scheme in Eqs. (15a)–(15b) or the divergence-preserving ADI method [94].

2.4. Fundamental Implicit Schemes for LOD-FDTD Methods with Three Split Matrices

Thus far, all the above fundamental implicit schemes have been involving only two split matrices (or their submatrices). There are implicit FDTD schemes that involve three split matrices of the Maxwell system matrix in Eq. (1a), i.e., $\mathbf{W} = \mathbf{A}_3 + \mathbf{B}_3 + \mathbf{C}_3$. One such scheme is also called the LOD-FDTD method and comprises three update procedures [95]:

$$\left(\mathbf{I} - \frac{\Delta t}{2}\mathbf{A}_3\right)\mathbf{u}^{n+\frac{1}{3}} = \left(\mathbf{I} + \frac{\Delta t}{2}\mathbf{A}_3\right)\mathbf{u}_1^n \tag{21a}$$

$$\left(\mathbf{I} - \frac{\Delta t}{2}\mathbf{B}_3\right)\mathbf{u}^{n+\frac{2}{3}} = \left(\mathbf{I} + \frac{\Delta t}{2}\mathbf{B}_3\right)\mathbf{u}^{n+\frac{1}{3}} \tag{21b}$$

$$\left(\mathbf{I} - \frac{\Delta t}{2}\mathbf{C}_3\right)\mathbf{u}_1^{n+1} = \left(\mathbf{I} + \frac{\Delta t}{2}\mathbf{C}_3\right)\mathbf{u}^{n+\frac{2}{3}}. \tag{21c}$$

$\mathbf{A}_3$, $\mathbf{B}_3$, and $\mathbf{C}_3$ are the split matrices that contain partial differential operators along x, y and z directions respectively as

$$\mathbf{A}_3 = \begin{bmatrix} 0 & 0 & 0 & 0 & 0 & 0 \\ 0 & 0 & 0 & 0 & 0 & \frac{-1}{\epsilon}\frac{\partial}{\partial x} \\ 0 & 0 & 0 & 0 & \frac{1}{\epsilon}\frac{\partial}{\partial x} & 0 \\ 0 & 0 & 0 & 0 & 0 & 0 \\ 0 & 0 & \frac{1}{\mu}\frac{\partial}{\partial x} & 0 & 0 & 0 \\ 0 & \frac{-1}{\mu}\frac{\partial}{\partial x} & 0 & 0 & 0 & 0 \end{bmatrix} \tag{22a}$$

$$\mathbf{B}_3 = \begin{bmatrix} 0 & 0 & 0 & 0 & 0 & \frac{1}{\epsilon}\frac{\partial}{\partial y} \\ 0 & 0 & 0 & 0 & 0 & 0 \\ 0 & 0 & 0 & \frac{-1}{\epsilon}\frac{\partial}{\partial y} & 0 & 0 \\ 0 & 0 & \frac{-1}{\mu}\frac{\partial}{\partial y} & 0 & 0 & 0 \\ 0 & 0 & 0 & 0 & 0 & 0 \\ \frac{1}{\mu}\frac{\partial}{\partial y} & 0 & 0 & 0 & 0 & 0 \end{bmatrix} \tag{22b}$$

$$\mathbf{C}_3 = \begin{bmatrix} 0 & 0 & 0 & 0 & \frac{-1}{\epsilon}\frac{\partial}{\partial z} & 0 \\ 0 & 0 & 0 & \frac{1}{\epsilon}\frac{\partial}{\partial z} & 0 & 0 \\ 0 & 0 & 0 & 0 & 0 & 0 \\ 0 & \frac{1}{\mu}\frac{\partial}{\partial z} & 0 & 0 & 0 & 0 \\ \frac{-1}{\mu}\frac{\partial}{\partial z} & 0 & 0 & 0 & 0 & 0 \\ 0 & 0 & 0 & 0 & 0 & 0 \end{bmatrix}. \tag{22c}$$

Note that the scheme in Eqs. (21a)–(21c) is only first-order accurate in time, hence the main field vectors (e.g., $\mathbf{u}_1^n$, $\mathbf{u}_1^{n+1}$) are subscripted '1' to signify the first-order temporal accuracy. To improve the efficiency, we again apply the principle of fundamental implicit schemes and obtain

$$\left(\frac{1}{2}\mathbf{I} - \frac{\Delta t}{4}\mathbf{A}_3\right)\mathbf{v}^{n+\frac{1}{3}} = \mathbf{u}_1^n, \quad \mathbf{u}^{n+\frac{1}{3}} = \mathbf{v}^{n+\frac{1}{3}} - \mathbf{u}_1^n \tag{23a}$$

$$\left(\frac{1}{2}\mathbf{I}-\frac{\Delta t}{4}\mathbf{B}_3\right)\mathbf{v}^{n+\frac{2}{3}}=\mathbf{u}^{n+\frac{1}{3}},\quad \mathbf{u}^{n+\frac{2}{3}}=\mathbf{v}^{n+\frac{2}{3}}-\mathbf{u}^{n+\frac{1}{3}} \tag{23b}$$

$$\left(\frac{1}{2}\mathbf{I}-\frac{\Delta t}{4}\mathbf{C}_3\right)\mathbf{v}^{n+1}=\mathbf{u}^{n+\frac{2}{3}},\quad \mathbf{u}_1^{n+1}=\mathbf{v}^{n+1}-\mathbf{u}^{n+\frac{2}{3}}. \tag{23c}$$

In these update procedures, all their RHS have been simplified in concise and efficient matrix-operator-free forms (no more $\mathbf{A}_3$, $\mathbf{B}_3$ or $\mathbf{C}_3$), thus resulting in simple, convenient coding and efficient implementation.

To increase the temporal accuracy from first to second order, some LOD-FDTD methods with three split matrices have been proposed that comprise five or more update procedures [96]. As an efficient alternative, we have developed the (fundamental) FLOD-FDTD method with three split matrices as [97]

$$\left(\frac{1}{2}\mathbf{I}-\frac{\Delta t}{4}\mathbf{A}_3\right)\mathbf{v}^{n,1}=\mathbf{u}^{n,0},\quad \mathbf{u}^{n,1}=\mathbf{v}^{n,1}-\mathbf{u}^{n,0} \tag{24a}$$

$$\left(\frac{1}{2}\mathbf{I}-\frac{\Delta t}{8}\mathbf{B}_3\right)\mathbf{v}^{n,2}=\mathbf{u}^{n,1},\quad \mathbf{u}^{n,2}=\mathbf{v}^{n,2}-\mathbf{u}^{n,1} \tag{24b}$$

$$\left(\frac{1}{2}\mathbf{I}-\frac{\Delta t}{4}\mathbf{C}_3\right)\mathbf{v}^{n,3}=\mathbf{u}^{n,2},\quad \mathbf{u}^{n,3}=\mathbf{v}^{n,3}-\mathbf{u}^{n,2} \tag{24c}$$

$$\left(\frac{1}{2}\mathbf{I}-\frac{\Delta t}{8}\mathbf{B}_3\right)\mathbf{v}^{n+1,0}=\mathbf{u}^{n,3},\quad \mathbf{u}^{n+1,0}=\mathbf{v}^{n+1,0}-\mathbf{u}^{n,3}. \tag{24d}$$

The main iterations consist of four implicit procedures with matrix-operator-free RHS for **ABCB** scheme in Eqs. (24a)–(24d), i.e., only one more compared to previous three for **ABC** scheme in Eqs. (23a)–(23c). Furthermore, the following input and output processings are to be performed:

$$\text{Input:}\quad \left(\frac{1}{2}\mathbf{I}+\frac{\Delta t}{8}\mathbf{A}_3\right)\mathbf{v}^{0,0}=\mathbf{u}^{0}_{\text{ABCB2}},\quad \mathbf{u}^{0,0}=\mathbf{v}^{0,0}-\mathbf{u}^{0}_{\text{ABCB2}} \tag{25a}$$

$$\text{Output:}\quad \left(\frac{1}{2}\mathbf{I}-\frac{\Delta t}{8}\mathbf{A}_3\right)\mathbf{v}^{n+1}=\mathbf{u}^{n+1,0},\quad \mathbf{u}^{n+1}_{\text{ABCB2}}=\mathbf{v}^{n+1}-\mathbf{u}^{n+1,0}. \tag{25b}$$

As before, these treatments will lead to second-order temporal-accurate main field vectors $\mathbf{u}^{n+1}_{\text{ABCB2}}$ (as signified by '2'). Note that the input processing in Eq. (25a) is required only once at the initial step for non-zero initial fields $\mathbf{u}^{0}_{\text{ABCB2}}$. The (infrequent) output processing in Eq. (25b) is to be performed independently of the main iterations only when the output data is needed. It may be bypassed altogether if we only need to output the field components along x direction, i.e., E_x and H_x. Besides **ABCB** scheme, the fundamental implicit schemes for other variants **BCAC** and **CABA**, as well as their reverse ones **BCBA**, **CACB**, and **ABAC** have also been developed [98]. All these schemes for FLOD-FDTD methods with three split matrices can be exploited to bypass the output processings for field components along various directions, thus achieving much simplicity and efficiency along with second-order temporal accuracy.

3. EM EDUCATIONAL MOBILE APPS

3.1. M1-D FDTD Methods for EM Educational Mobile Apps

Exploiting the wide accessibility of mobile devices, several educational mobile apps have been created for enhanced teaching and learning of electromagnetics [9–14]. They provide touch-based interactivity and real-time EM+circuit simulations as well as 2-D/3-D visualizations of wave phenomena. Fig. 1 shows the educational mobile apps on Android phones for (a) EM wave polarization and (b) plane wave reflection and transmission. To bypass the intensive full-wave 3-D computations, we have proposed multiple 1-D (M1-D) FDTD methods, which are useful for quick initial design, analysis and seamless teaching/learning, etc. Like the 3-D counterparts, the M1-D FDTD methods may involve explicit and/or implicit update procedures. The M1-D explicit FDTD method consists of simple multiple 1-D update

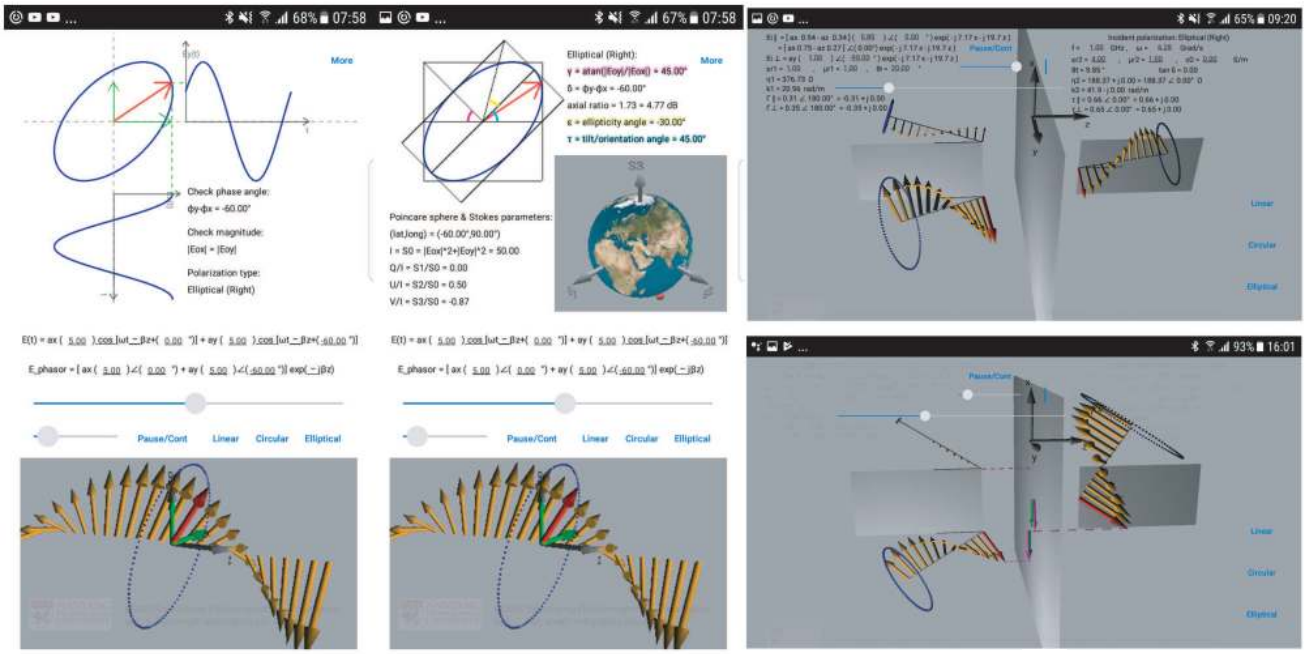

Figure 1. Educational mobile apps on Android phones for (a) EM wave polarization and (b) plane wave reflection and transmission.

equations, which can be readily implemented for transmission line (TL) mobile app [9]. Such mobile app allows user-friendly touch-based interactivity and user-configurable simulation parameters. It allows instructors and students to construct practical microstrip circuits including multiple TLs, open-/short-circuited stubs, as well as lumped elements such as resistors, capacitors and inductors in parallel and/or series. The TLs and stubs including lumped elements are modeled using effective permittivity and characteristic impedance, along with electric and (unconventional) magnetic current concepts. Based on the constructed TL circuits and their effective modeling, simulations of wave propagations can be performed efficiently on mobile devices. These simulations are useful to provide ubiquitous and real-time visualizations for mobile interactive teaching and learning of TL concepts anytime, anywhere [99].

3.2. M1-D FADI-FDTD Method for Multiple Transmission Lines and Stubs

The M1-D explicit FDTD method above is conditionally stable with its time step size restricted by certain stability constraint, which is more stringent than that of the pure 1-D FDTD method. The stability constraint limits the simulation efficiency and may require students' long wait for observing various phenomena demonstrations, e.g., wave reflections on long TLs and stubs. To improve the efficiency, we have developed the unconditionally stable M1-D FADI-FDTD method. Such method involves one-step update procedures for main TL and stub as [100, 101]

– Main TL:

$$\mathbf{B}_m = \begin{bmatrix} 0 & \frac{-1}{\epsilon_m}\frac{\partial}{\partial z} \\ \frac{-1}{\mu_m}\frac{\partial}{\partial z} & 0 \end{bmatrix}, \quad \mathbf{u}_m^{n+1} = \begin{bmatrix} E_{x,m}^{n+1} \\ H_{y,m}^{n+1} \end{bmatrix} \tag{26a}$$

$$\left(\frac{1}{2}\mathbf{I} - \frac{\Delta t}{4}\mathbf{B}_m\right)\mathbf{v}_m^{n+1} = \mathbf{u}_m^n, \quad \mathbf{u}_m^{n+1} = \mathbf{v}_m^{n+1} - \mathbf{u}_m^n; \tag{26b}$$

– Stub:

$$\mathbf{A}_s = \begin{bmatrix} 0 & \frac{1}{\epsilon_s}\frac{\partial}{\partial y} \\ \frac{1}{\mu_s}\frac{\partial}{\partial z} & 0 \end{bmatrix}, \quad \mathbf{u}_s^{n+\frac{1}{2}} = \begin{bmatrix} E_{x,s}^{n+\frac{1}{2}} \\ H_{z,s}^{n+\frac{1}{2}} \end{bmatrix} \tag{27a}$$

$$\left(\frac{1}{2}\mathbf{I} - \frac{\Delta t}{4}\mathbf{A}_s\right)\mathbf{v}_s^{n+\frac{1}{2}} = \mathbf{u}_s^{n-\frac{1}{2}}, \quad \mathbf{u}_s^{n+\frac{1}{2}} = \mathbf{v}_s^{n+\frac{1}{2}} - \mathbf{u}_s^{n-\frac{1}{2}}. \tag{27b}$$

Notice that $\mathbf{B}_m$ and $\mathbf{A}_s$ are the sole 2×2 matrix operators for main TL and stub in Eqs. (26a) and (27a) respectively. The RHS of Eqs. (26b) and (27b) are matrix-operator-free without any spatial derivative, which simplify the implementations and improve the efficiency of implicit update procedures.

At the interjunctions between multiple TLs and stubs, there is a need to relate their EM fields using proper source treatments via current densities (without which may cause instability):

$$J_x^m = -\frac{\partial}{\partial y}H_z^s, \quad J_x^s = \frac{\partial}{\partial z}H_y^m. \tag{28}$$

Using the M1-D FADI-FDTD method along with these source treatments, the EM fields in all interconnected main TLs and stubs can be updated cooperatively and efficiently to solve practical circuits. Fig. 2 shows the simulations of wave propagations on iPad for (a) TL with open-/short-circuited stubs and (b) branch line coupler using M1-D FADI-FDTD method. The simulations can be accelerated by adjusting the time step size using the slider on the iPad app. Note that the time step size is specified in terms of $\text{CFLN} = \Delta t/\Delta t_{\text{CFL}}$. With the unconditional stability of FADI methods, the simulations are 'fast-forwardable' with enhanced efficiency by using $\text{CFLN} > 1$, e.g., $\text{CFLN} = 10, 16$, etc. This is very useful for quick concept illustrations or phenomena demonstrations, skipping uninteresting details during interactive teaching and learning. Alternative to FADI, one may also resort to the FLOD FDTD method with non-uniform time-steps for more trade-offs between efficiency and accuracy [102].

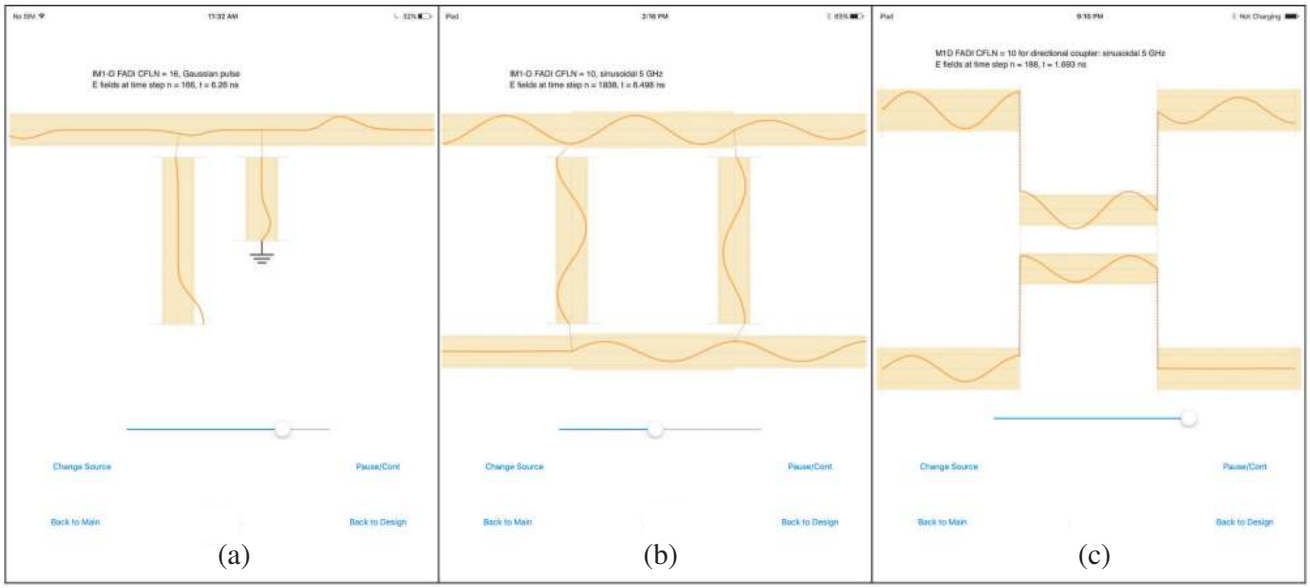

Figure 2. Simulations of wave propagations on iPad for (a) TL with open-/short-circuited stubs, (b) branch line coupler and (c) directional coupler using M1-D FADI FDTD and CL-FDTD methods.

3.3. M1-D FADI CL-FDTD Method for Coupled Transmission Lines

For coupled transmission lines, the EM fields are governed by alternative differential equations, which are different from the usual Maxwell's equations and can be written as [103, 104],

$$\frac{\partial \mathbf{u}_{\text{cl}}}{\partial t} = \mathbf{W}_{\text{cl}}\mathbf{u}_{\text{cl}}, \quad \mathbf{u}_{\text{cl}} = [E_{x1}, \quad E_{x2}, \quad H_{y1}, \quad H_{y2}]^T \tag{29a}$$

$$\mathbf{W}_{\text{cl}} = \begin{bmatrix} 0 & 0 & \frac{-1}{\epsilon_s}\frac{\partial}{\partial z} & \frac{-1}{\epsilon_m}\frac{\partial}{\partial z} \\ 0 & 0 & \frac{-1}{\epsilon_m}\frac{\partial}{\partial z} & \frac{-1}{\epsilon_s}\frac{\partial}{\partial z} \\ \frac{-1}{\mu_s}\frac{\partial}{\partial z} & \frac{1}{\mu_m}\frac{\partial}{\partial z} & 0 & 0 \\ \frac{1}{\mu_m}\frac{\partial}{\partial z} & \frac{-1}{\mu_s}\frac{\partial}{\partial z} & 0 & 0 \end{bmatrix}. \tag{29b}$$

$\mathbf{W}_{\text{cl}}$ is the 4×4 coupled line (CL) system matrix, and E_{x1}, H_{y1} are the EM fields along line 1, while E_{x2}, H_{y2} are those along line 2. ϵ_s, ϵ_m and μ_s, μ_m are the self and mutual permittivities and permeabilities, respectively, which can be expressed in terms of CL even- and odd-mode characteristic impedances (Z_{0e}, Z_{0o}), phase velocities (v_e, v_o) and effective permittivities (ϵ^e_{eff}, ϵ^o_{eff}) [105–107]. Equations (29a)–(29b) can be solved using the M1-D CL-FDTD method [103, 104], which could bypass the fine mesh for line width and spacing of coupled transmission lines. However, due to the stability constraint of such explicit method for CL, there is a time step limit that is usually more restrictive than that for the single uncoupled TL.

The CL system matrix $\mathbf{W}_{\text{cl}}$ can be expressed as the sum of some split matrices $\mathbf{A}_{\text{cl}}$ and $\mathbf{B}_{\text{cl}}$. Using these split matrices, the M1-D FADI CL-FDTD method can be formulated for coupled transmission lines as

$$\mathbf{v}^n_{\text{cl}} = \mathbf{u}^n_{\text{cl}} - \mathbf{v}^{n-\frac{1}{2}}_{\text{cl}}, \quad \left(\frac{1}{2}\mathbf{I} - \frac{\Delta t}{4}\mathbf{A}_{\text{cl}}\right)\mathbf{u}^{n+\frac{1}{2}}_{\text{cl}} = \mathbf{v}^n_{\text{cl}} \tag{30a}$$

$$\mathbf{v}^{n+\frac{1}{2}}_{\text{cl}} = \mathbf{u}^{n+\frac{1}{2}}_{\text{cl}} - \mathbf{v}^n_{\text{cl}}, \quad \left(\frac{1}{2}\mathbf{I} - \frac{\Delta t}{4}\mathbf{B}_{\text{cl}}\right)\mathbf{u}^{n+1}_{\text{cl}} = \mathbf{v}^{n+\frac{1}{2}}_{\text{cl}}. \tag{30b}$$

While the RHS of Eqs. (30a)–(30b) are matrix-operator-free, the split matrices should be chosen such that the LHS would result in tridiagonal matrices that can be solved efficiently. Moreover, they must maintain the stability of M1-D FADI CL-FDTD method even for time step size larger than the CFL constraint. Many sets of split matrices have been proposed and investigated further [108–111]. Some of them have been found to be unstable including the natural set with self-mutual separation, which follows the direct way of splitting and reduces naturally to the uncoupled case when all mutual terms are omitted. Two sets of split matrices that have been found to be resulting in stable schemes with tridiagonal matrices are given below (subscripted 'cl1' and 'cl2' for set 1 and 2):

$$\mathbf{W}_{\text{cl}} = \mathbf{A}_{\text{cl1}} + \mathbf{B}_{\text{cl1}} = \mathbf{A}_{\text{cl2}} + \mathbf{B}_{\text{cl2}} \tag{31}$$

$$\mathbf{A}_{\text{cl1}} = \begin{bmatrix} 0 & 0 & \frac{-1}{\epsilon_s}\frac{\partial}{\partial z} & 0 \\ 0 & 0 & \frac{-1}{\epsilon_m}\frac{\partial}{\partial z} & 0 \\ \frac{-1}{\mu_s}\frac{\partial}{\partial z} & 0 & 0 & 0 \\ \frac{1}{\mu_m}\frac{\partial}{\partial z} & 0 & 0 & 0 \end{bmatrix}, \quad \mathbf{B}_{\text{cl1}} = \begin{bmatrix} 0 & 0 & 0 & \frac{-1}{\epsilon_m}\frac{\partial}{\partial z} \\ 0 & 0 & 0 & \frac{-1}{\epsilon_s}\frac{\partial}{\partial z} \\ 0 & \frac{1}{\mu_m}\frac{\partial}{\partial z} & 0 & 0 \\ 0 & \frac{-1}{\mu_s}\frac{\partial}{\partial z} & 0 & 0 \end{bmatrix} \tag{32}$$

$$\mathbf{A}_{\text{cl2}} = \begin{bmatrix} 0 & 0 & \frac{-1}{\epsilon_s}\frac{\partial}{\partial z} & \frac{-1}{\epsilon_m}\frac{\partial}{\partial z} \\ 0 & 0 & 0 & 0 \\ \frac{-1}{\mu_s}\frac{\partial}{\partial z} & \frac{1}{\mu_m}\frac{\partial}{\partial z} & 0 & 0 \\ 0 & 0 & 0 & 0 \end{bmatrix}, \quad \mathbf{B}_{\text{cl2}} = \begin{bmatrix} 0 & 0 & 0 & 0 \\ 0 & 0 & \frac{-1}{\epsilon_m}\frac{\partial}{\partial z} & \frac{-1}{\epsilon_s}\frac{\partial}{\partial z} \\ 0 & 0 & 0 & 0 \\ \frac{1}{\mu_m}\frac{\partial}{\partial z} & \frac{-1}{\mu_s}\frac{\partial}{\partial z} & 0 & 0 \end{bmatrix}. \tag{33}$$

Figure 2(c) shows the simulations of wave propagations on iPad for directional coupler using M1-D FADI CL-FDTD method. The simulations of the coupled transmission lines (with uncoupled TLs at both input and output sections) provide much intuitional insight for understanding wave propagations in time domain [112]. Alternative to ADI, one may also resort to the multiple LOD coupled line FDTD methods, noting the proper split matrices for stability and efficiency [113, 114].

3.4. Further Developments and Extensions of Mobile Apps

Thus far, only time-domain methods have been discussed for CEM and mobile apps. Besides time domain, we have also developed many (unconditionally) stable and efficient frequency-domain methods

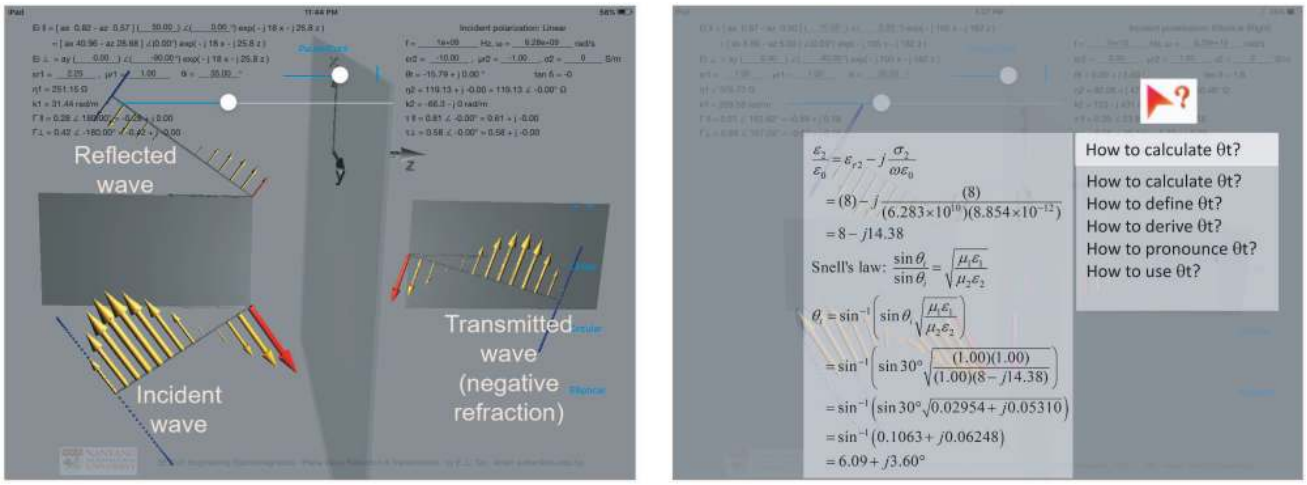

(a) (b)

Figure 3. a) Snapshot on iPad for plane wave incident upon a double negative medium demonstrating negative refraction. (b) Illustration of mobile ITS with intelligent step-by-step guide to calculate the angle of transmission θ_t in a lossy medium.

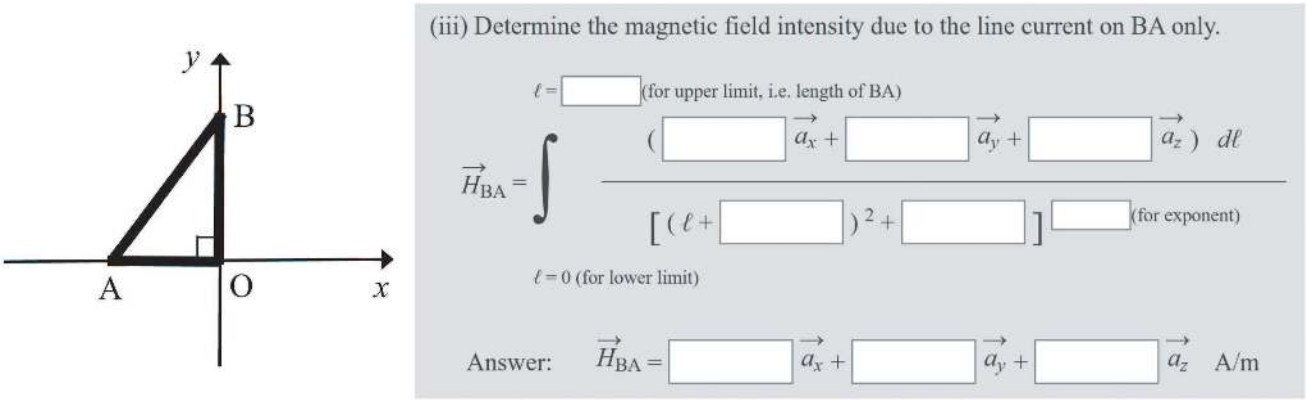

Figure 4. Sample online question involving integration and vector components for determining the magnetic field due to a particular line current at certain observation point.

including scattering [115–117], impedance [118] and hybrid [119, 120] matrix methods. These frequency-domain methods are well-suited for further developments of useful mobile apps as well, e.g., calculations of S parameters, illustrations of wave polarization, reflection and transmission, etc. More advanced analyses can be carried out on mobile apps for EM waves in various complex media including biisotropic [121–123], anisotropic [124–126], gyrotropic [127, 128] and bianisotropic [129–133] media, etc. For illustration, Fig. 3(a) shows the snapshot on iPad for plane wave incident upon a double negative medium demonstrating negative refraction. The frequency-domain methods on mobile apps can also be extended for further research and applications beyond electromagnetics, such as optics (diffraction gratings, photonic crystals) [134–136], acoustics (phononic crystals, elastic, anisotropic and piezoelectric media) [137–144], circuits (geometrical [145–148], Rollett-based [149, 150] and quasi-invariant stability [151–153], pole-zero [154–156], energy consideration [157–159]), etc. Apart from providing seamless interactive simulations and insightful visualizations, our educational mobile apps may be enhanced with artificial intelligence (AI) via innovative mobile intelligent tutoring systems (ITS). Fig. 3(b) shows the illustration of mobile ITS with intelligent step-by-step guide to calculate the angle of transmission θ_t in a lossy medium. Such guide should be very helpful for some weak students who might need to

learn the square root or arcsin of a complex number. In addition to tutoring, more thorough and rigorous assessments may also be incorporated onto online/mobile platforms. Fig. 4 shows a sample online question involving integration and vector components for determining the magnetic field due to a particular line current at certain observation point, which may be randomly set for individual students to deter cheating or copying. Such assessments enable the capturing and auto-marking of students' key intermediate workings in addition to their final answers, thus paving the way for comprehensive online or paperless examinations for electromagnetics and other math-intensive courses.

4. CONCLUSION

This paper has presented an overview and review of the fundamental implicit FDTD schemes for CEM and educational mobile apps. The fundamental implicit FDTD schemes are unconditionally stable and feature the most concise update procedures with matrix-operator-free RHS, which are simpler and more efficient than all previous implicit schemes having RHS matrix operators. They constitute the basis of unification for many implicit schemes including classical ones, providing insights into their inter-relations along with simplifications, concise updates and efficient implementations. The classical schemes as well as ADI-, SS-, and LOD-FDTD methods with two or three split matrices, etc., can all be simplified into concise and efficient forms with matrix-operator-free RHS. Based on the fundamental implicit schemes, further developments can be carried out more conveniently including extensions to other branches of physics. To simulate multiple transmission lines, stubs and coupled transmission lines efficiently, the M1-D explicit FDTD method and the unconditionally stable M1-D FADI FDTD and CL-FDTD methods have been discussed. With the unconditional stability of FADI methods, the simulations are fast-forwardable with enhanced efficiency. This is very useful for quick concept illustrations or phenomena demonstrations during interactive teaching and learning. Besides time domain, many frequency-domain methods are well-suited for further developments of useful mobile apps as well. They can also be extended for further research and applications in electromagnetics and beyond.

REFERENCES

1. Taflove, A. and S. C. Hagness, *Computational Electrodynamics: The Finite-Difference Time-Domain Method*, Artech House, Boston, M.A., 2005.
2. Yee, K. S., "Numerical solution of initial boundary value problems involving Maxwell's equations in isotropic media," *IEEE Trans. Antennas Propag.*, Vol. 14, No. 3, 302–307, 1966.
3. Zheng, F., Z. Chen, and J. Zhang, "Toward the development of a three-dimensional unconditionally stable finite-difference time-domain method," *IEEE Trans. Microw. Theory Tech.*, Vol. 48, No. 9, 1550–1558, 2000.
4. Namiki, T., "3-D ADI-FDTD method — Unconditionally stable time-domain algorithm for solving full vector Maxwell's equations," *IEEE Trans. Microw. Theory Tech.*, Vol. 48, 1743–1748, 2000.
5. Fu, W. and E. L. Tan, "Development of split-step FDTD method with higher order spatial accuracy," *Electron. Lett.*, Vol. 40, No. 20, 1252–1254, 2004.
6. Fu, W. and E. L. Tan, "Compact higher-order split-step FDTD method," *Electron. Lett.*, Vol. 41, No. 7, 397–399, 2005.
7. Tan, E. L., "Unconditionally stable LOD-FDTD method for 3-D Maxwell's equations," *IEEE Microw. Wireless Compon. Lett.*, Vol. 17, No. 2, 85–87, 2007.
8. Tan, E. L., "Fundamental schemes for efficient unconditionally stable implicit finite-difference time-domain methods," *IEEE Trans. Antennas Propag.*, Vol. 56, No. 1, 170–177, 2008.
9. Yang, Z. and E. L. Tan, "A microstrip circuit tool kit app with FDTD analysis including lumped elements," *IEEE Microw. Mag.*, Vol. 16, No. 1, 74–80, 2015.
10. Yang, Z. and E. L. Tan, "A microwave transmission line courseware based on multiple 1-D FDTD method on mobile devices," *Asia-Pacific Conf. Antennas Propag.*, 251–252, Bali, 2015.
11. Tan, E. L. and D. Y. Heh, "Demonstration of electromagnetic polarization app on iPad," *IEEE Int. Conf. Comput. Electromagn.*, 196–197, Kumamoto, 2017.

12. Tan, E. L. and D. Y. Heh, "Mobile device aided teaching and learning of electromagnetic polarization," *IEEE Int. Conf. Teaching, Assessment, and Learning for Engineering*, 52–55, Hong Kong, 2017.
13. Tan, E. L. and D. Y. Heh, "Teaching and learning electromagnetic polarization using mobile devices," *IEEE Antennas Propag. Mag.*, Vol. 60, No. 4, 112–121, 2018.
14. Tan, E. L. and D. Y. Heh, "Teaching and learning electromagnetic plane wave reflection and transmission using 3-D TV," *IEEE Antennas Propag. Mag.*, Vol. 61, No. 2, 101–108, 2019.
15. Peaceman, D. and H. Rachford, Jr., "The numerical solution of parabolic and elliptic differential equations," *J. Soc. Ind. Appl. Math.*, Vol. 3, No. 1, 28–41, 1955.
16. Mitchell, A. R. and D. F. Griffiths, *The Finite-Difference Method in Partial Differential Equations*, Wiley, New York, 1980.
17. Thomas, J. W., *Numerical Partial Differential Equations: Finite Difference Methods*, Springer-Verlag, New York, 1998.
18. Tan, E. L., "Efficient algorithm for the unconditionally stable 3-D ADI-FDTD method," *IEEE Microw. Wireless Compon. Lett.*, Vol. 17, No. 1, 7–9, 2007.
19. Tan, E. L., "Concise current source implementation for efficient 3-D ADI-FDTD method," *IEEE Microw. Wireless Compon. Lett.*, Vol. 17, No. 11, 748–750, 2007.
20. Douglas, J., "Alternating direction methods for three space variables," *Numerische Mathematik*, Vol. 4, No. 1, 94–102, 1962.
21. Sun, G. and C. W. Trueman, "Efficient implementations of the Crank-Nicolson scheme for the finite-difference time-domain method," *IEEE Trans. Microw. Theory Tech.*, Vol. 54, No. 5, 2275–2284, 2006.
22. Tan, E. L., "Efficient algorithms for Crank-Nicolson-based finite-difference time-domain methods," *IEEE Trans. Microw. Theory Tech.*, Vol. 56, No. 2, 408–413, 2008.
23. Fu, W. and E. L. Tan, "Stability and dispersion analysis for higher order 3-D ADI-FDTD method," *IEEE Trans. Antennas Propag.*, Vol. 53, No. 11, 3691–3696, 2005.
24. Fu, W. and E. L. Tan, "A compact higher-order ADI-FDTD method," *Microwave Opt. Technol. Lett.*, Vol. 44, No. 3, 273–275, 2005.
25. Fu, W. and E. L. Tan, "A parameter optimized ADI-FDTD method based on the (2,4) stencil," *IEEE Trans. Antennas Propag.*, Vol. 54, No. 6, 1836–1842, 2006.
26. Fu, W. and E. L. Tan, "Stability and dispersion analysis for ADI-FDTD method in lossy media," *IEEE Trans. Antennas Propag.*, Vol. 55, No. 4, 1095–1102, 2007.
27. Singh, G., E. L. Tan, and Z. N. Chen, "Efficient tensor based FDTD scheme for modeling sloped interfaces in lossy media," *Microwave Opt. Technol. Lett.*, Vol. 51, No. 6, 1530–1537, 2009.
28. Heh, D. Y. and E. L. Tan, "Dispersion analysis of FDTD schemes for doubly lossy media," *Progress In Electromagnetics Research B*, Vol. 17, 327–342, 2009.
29. Heh, D. Y. and E. L. Tan, "Generalized stability criterion of 3-D FDTD schemes for doubly lossy media," *IEEE Trans. Antennas Propag.*, Vol. 58, No. 4, 1421–1425, 2010.
30. Heh, D. Y. and E. L. Tan, "Lyapunov and matrix norm stability analysis of ADI-FDTD schemes for doubly lossy media," *IEEE Trans. Antennas Propag.*, Vol. 59, No. 3, 979–986, 2011.
31. Heh, D. Y. and E. L. Tan, "Efficient implementation of 3-D ADI-FDTD method for lossy media," *IEEE MTT-S Int. Microwave Symp.*, 313–316, Boston, Massachusetts, 2009.
32. Heh, D. Y. and E. L. Tan, "Unified efficient fundamental ADI-FDTD schemes for lossy media," *Progress In Electromagnetics Research B*, Vol. 32, 217–242, 2011.
33. Fu, W. and E. L. Tan, "Effective permittivity scheme for ADI-FDTD method at the interface of dispersive media," *Appl. Comput. Electromag. Soc. J.*, Vol. 23, No. 2, 120–125, 2008.
34. Heh, D. Y. and E. L. Tan, "Modeling Lorentz dispersive media in FDTD using the exponential time differencing method," *Asia-Pacific Microwave Conf.*, Hong Kong, 2008.
35. Heh, D. Y. and E. L. Tan, "FDTD modeling for dispersive media using matrix exponential method," *IEEE Microw. Wireless Compon. Lett.*, Vol. 19, No. 2, 53–55, 2009.

36. Tan, E. L. and D. Y. Heh, "Corrected impulse invariance method for dispersive media using FDTD," *Asia-Pacific Symp. Electromag. Compat.*, 56–59, Singapore, 2008.
37. Heh, D. Y. and E. L. Tan, "Corrected impulse invariance method in Z-transform theory for frequency-dependent FDTD methods," *IEEE Trans. Antennas Propag.*, Vol. 57, No. 9, 2683–2690, 2009.
38. Heh, D. Y. and E. L. Tan, "Modeling Debye dispersive media using efficient ADI-FDTD method," *IEEE AP-S Int. Symp. Antennas Propag.*, Charleston, 2009.
39. Heh, D. Y. and E. L. Tan, "Fundamental ADI-FDTD method for multiple-pole Debye dispersive media," *Asia-Pacific Conf. Antennas Propag.*, 9–10, Singapore, 2012.
40. Heh, D. Y. and E. L. Tan, "Stable formulation of FADI-FDTD method for multiterm, doubly, second-order dispersive media," *IEEE Trans. Antennas Propag.*, Vol. 61, No. 8, 4167–4175, 2013.
41. Heh, D. Y. and E. L. Tan, "Unconditionally stable fundamental alternating direction implicit FDTD method for dispersive media," *Computational Electromagnetics — Retrospective and Outlook*, Chapter 4, 85–116, Springer, 2015.
42. Heh, D. Y. and E. L. Tan, "Modeling hemoglobin at optical frequency using the unconditionally stable fundamental ADI-FDTD method," *Biomedical Opt. Expr.*, Vol. 2, No. 5, 1169–1183, 2011.
43. Heh, D. Y. and E. L. Tan, "Modeling the interaction of terahertz pulse with healthy skin and basal cell carcinoma using the unconditionally stable fundamental ADI-FDTD method," *Progress In Electromagnetics Research B*, Vol. 37, 365–386, 2012.
44. Fu, W. and E. L. Tan, "ADI-FDTD method including linear lumped networks," *Electron. Lett.*, Vol. 42, No. 13, 728–729, 2006.
45. Fu, W. and E. L. Tan, "Unconditionally stable FDTD technique including passive lumped elements," *2006 Int. RF Microwave Conf.*, Putrajaya, Malaysia, 2006.
46. Fu, W. and E. L. Tan, "Unconditionally stable ADI-FDTD method including passive lumped elements," *IEEE Trans. Electromagn. Compat.*, Vol. 48, No. 4, 661–668, 2006.
47. Gan, T. H., Z. Yang and E. L. Tan, "A polarization-reconfigurable filtering antenna system," *IEEE Antennas Propag. Mag.*, Vol. 55, No. 6, 198–219, 2013.
48. Yang, Z. and E. L. Tan, "A de-embedding technique for diode-incorporated reconfigurable antenna simulation," *IEEE AP-S Int. Symp. Antennas Propag.*, 1437–1438, Farjardo, Puerto Rico, 2016.
49. Yang, Z. and E. L. Tan, "A fundamental ADI-FDTD method with implicit update for magnetic fields in the second procedure," *Asia-Pacific Conf. Antennas Propag.*, 6–7, Bali, 2015.
50. Tay, W. C. and E. L. Tan, "Implementation of Mur first order absorbing boundary condition in efficient 3-D ADI-FDTD," *IEEE AP-S Int. Symp. Antennas Propag.*, Charleston, 2009.
51. Tay, W. C. and E. L. Tan, "Split-field PML implementation for the efficient fundamental ADI-FDTD method," *Asia-Pacific Microwave Conf.*, 1553–1556, Singapore, 2009.
52. Singh, G., E. L. Tan and Z. N. Chen, "Analytic fields of a focused beam with higher-order compensations for FDTD TF/SF formulation," *IEEE AP-S Int. Symp. Antennas Propag.*, 2278–2281, Spokane, 2011.
53. Singh, G., E. L. Tan and Z. N. Chen, "Analytic fields with higher-order compensations for 3-D FDTD TF/SF formulation with application to beam excitations," *IEEE Trans. Antennas Propag.*, Vol. 59, No. 7, 2588–2598, 2011.
54. Gan, T. H. and E. L. Tan, "An efficient total-field/scattered-field technique for the fundamental ADI-FDTD method," *IEEE AP-S Int. Symp. Antennas Propag.*, 159–160, Memphis, 2014.
55. Singh, G., E. L. Tan, and Z. N. Chen, "Efficient complex envelope ADI-FDTD method for the analysis of anisotropic photonic crystals," *IEEE Photon. Technol. Lett.*, Vol. 23, No. 12, 801–803, 2011.
56. Singh, G., E. L. Tan, and Z. N. Chen, "Modeling magnetic photonic crystals with lossy ferrites using efficient complex envelope ADI-FDTD method," *Opt. Lett.*, Vol. 36, No. 8, 1494–1496, 2011.
57. D'Yakonov, Ye. G., "On some difference schemes for solutions of boundary problems," *U.S.S.R. Comput. Math. and Math. Phys.*, Vol. 2, 55–77, 1962.

58. Shibayama, J., T. Hirano, J. Yamauchi, and H. Nakano, "Efficient implementation of frequency-dependent 3D LOD-FDTD method using fundamental scheme," *Electron. Lett.*, Vol. 48, No. 13, 774–775, 2012.
59. Yang, Z., E. L. Tan, and L. Wang, "Upgrading LOD-FDTD method to efficient method with second-order accuracy," *Asia-Pacific Microwave Conf.*, Nanjing, 2015.
60. Gan, T. H. and E. L. Tan, "Unconditionally stable fundamental LOD-FDTD method with second-order temporal accuracy and complying divergence," *IEEE Trans. Antennas Propag.*, Vol. 61, No. 5, 2630–2638, 2013.
61. Gan, T. H. and E. L. Tan, "Convolutional perfectly matched layer (CPML) for fundamental LOD-FDTD method with 2nd order temporal accuracy and complying divergence," *Asia-Pacific Microwave Conf.*, 839–841, Seoul, Korea, 2013.
62. Gan, T. H. and E. L. Tan, "Application of the fundamental LOD2-CD-FDTD method for antenna modeling," *Asia-Pacific Conf. Antennas Propag.*, 445–446, Bali, 2015.
63. Gan, T. H. and E. L. Tan, "Current source implementations for fundamental SS2-FDTD method," *Asia-Pacific Microwave Conf.*, 1292–1294, Kaohsiung, 2012.
64. Heh, D. Y. and E. L. Tan, "Split-step finite-difference time-domain method with fourth order accuracy in time," *Asia-Pacific Symp. Electromag. Compat.*, 68–71, Singapore, 2008.
65. Tan, E. L. and D. Y. Heh, "ADI-FDTD method with fourth order accuracy in time," *IEEE Microw. Wireless Compon. Lett.*, Vol. 18, No. 5, 296–298, 2008.
66. Heh, D. Y. and E. L. Tan, "Further reinterpretation of multi-stage implicit FDTD schemes," *IEEE Trans. Antennas Propag.*, Vol. 62, No. 8, 4407–4411, 2014.
67. Garcia, S. G., T. W. Lee, and S. C. Hagness, "On the accuracy of the ADI-FDTD method," *IEEE Antennas Wireless Propag. Lett.*, Vol. 1, 31–34, 2002.
68. Kong, Y. and Q. Chu, "High-order split-step unconditionally-stable FDTD methods and numerical analysis," *IEEE Trans. Antennas Propag.*, Vol. 59, No. 9, 3280–3289, 2011.
69. Tan, E. L., "Acceleration of LOD-FDTD method using fundamental scheme on graphics processor units," *IEEE Microw. Wireless Compon. Lett.*, Vol. 20, No. 12, 648–650, 2010.
70. Tay, W. C., D. Y. Heh, and E. L. Tan, "GPU-accelerated fundamental ADI-FDTD with complex frequency shifted convolutional perfectly matched layer," *Progress In Electromagnetics Research M*, Vol. 14, 177–192, 2010.
71. Tay, W. C. and E. L. Tan, "Mur absorbing condition for efficient fundamental 3D LOD-FDTD," *IEEE Microw. Wireless Compon. Lett.*, Vol. 20, No. 2, 61–63, 2010.
72. Tay, W. C. and E. L. Tan, "Implementations of PMC and PEC boundary conditions for efficient fundamental ADI and LOD-FDTD," *Journal of Electromagnetic Waves and Applications*, Vol. 24, No. 4, 565–573, 2010.
73. Singh, G., E. L. Tan, and Z. N. Chen, "Implementation of total-field/scattered-field technique in the 2-D LOD-FDTD method," *Asia-Pacific Microwave Conf.*, 1505–1508, Singapore, 2009.
74. Singh, G., E. L. Tan, and Z. N. Chen, "A split-step FDTD method for 3-D Maxwell's equations in general anisotropic media," *IEEE Trans. Antennas Propag.*, Vol. 58, No. 11, 3647–3657, 2010.
75. Heh, D. Y. and E. L. Tan, "Complex-envelope LOD-FDTD method for ionospheric propagation," *IEEE AP-S Int. Symp. Antennas Propag.*, 2027–2028, Farjardo, Puerto Rico, 2016.
76. Yang, Z. and E. L. Tan, "Efficient 3-D fundamental LOD-FDTD method with lumped elements," *IEEE MTT-S Int. Microwave Symp.*, Tampa, 2014.
77. Yang, Z. and E. L. Tan, "3-D unified FLOD-FDTD method incorporated with lumped elements," *IEEE AP-S Int. Symp. Antennas Propag.*, San Diego, 2017.
78. Yang, Z. and E. L. Tan, "Two finite-difference time-domain methods incorporated with memristor," *Progress In Electromagnetics Research M*, Vol. 42, 153–158, 2015.
79. Yang, Z. and E. L. Tan, "Efficient 3-D fundamental LOD-FDTD method incorporated with memristor," *IEICE Trans. Electronics*, Vol. E99-C, No. 7, 788–792, 2016.
80. Yang, Z. and E. L. Tan, "3-D non-uniform time step locally onedimensional FDTD method," *Electron. Lett.*, Vol. 52, No. 12, 993–994, 2016.

81. Yang, Z. and E. L. Tan, "Stability analyses of non-uniform time-step schemes for ADI- and LOD-FDTD methods," *IEEE Int. Conf. Comput. Electromagn.*, 312–313, Kumamoto, 2017.
82. Tan, E. L. and D. Y. Heh, "Stability analyses of nonuniform time-step LOD-FDTD methods for electromagnetic and thermal simulations," *IEEE J. Multiscale Multiphys. Comput. Tech.*, Vol. 2, 183–193, 2017.
83. Heh, D. Y. and E. L. Tan, "Some recent developments in fundamental implicit FDTD schemes," *Asia-Pacific Symp. Electromag. Compat.*, 153–156, Singapore, 2012.
84. Tay, W. C. and E. L. Tan, "Efficient algorithm for 3-D thermal alternating-direction-implicit method," *IEEE Electrical Design Adv. Packag. Syst. Symp.*, 177–180, Taipei, 2012.
85. Tay, W. C., E. L. Tan, and D. Y. Heh, "Fundamental locally one-dimensional method for 3-D thermal simulation," *IEICE Trans. Electronics*, Vol. E97-C, No. 7, 636–644, 2014.
86. Heh, D. Y., E. L. Tan, and W. C. Tay, "Fast alternating direction implicit method for efficient transient thermal simulation of integrated circuits," *Int. J. Numer. Model. Electron. Networks Devices Fields*, Vol. 29, No. 1, 93–108, 2016.
87. Tay, W. C. and E. L. Tan, "Pentadiagonal alternating-direction-implicit finite-difference time-domain method for two-dimensional Schrödinger equation," *Computer Phys. Comm.*, Vol. 185, No. 7, 1886–1892, 2014.
88. Cooke, S. J., M. Botton, T. M. Antonsen, and B. Levush, "A leapfrog formulation of the 3D ADI-FDTD algorithm," *Int. J. Numer. Model*, Vol. 22, No. 2, 187–200, 2009.
89. Gan, T. H. and E. L. Tan, "Stability and dispersion analysis for three-dimensional (3-D) leapfrog ADI-FDTD method," *Progress In Electromagnetics Research M*, Vol. 23, 1–12, 2012.
90. Gan, T. H. and E. L. Tan, "Divergence of electric field for the two-dimensional (2-D) leapfrog ADI-FDTD method," *IEEE AP-S Int. Symp. Antennas Propag.*, Chicago, 2012.
91. Gan, T. H. and E. L. Tan, "Analysis of the divergence properties for the three-dimensional leapfrog ADI-FDTD method," *IEEE Trans. Antennas Propag.*, Vol. 60, No. 12, 5801–5808, 2012.
92. Gan, T. H. and E. L. Tan, "Unconditionally stable leapfrog ADI-FDTD method for lossy media," *Progress In Electromagnetics Research M*, Vol. 26, 173–186, 2012.
93. Gan, T. H. and E. L. Tan, "On the field leakage of the leapfrog ADI-FDTD method for nonpenetrable targets," *Microwave Opt. Technol. Lett.*, Vol. 56, No. 6, 1401–1405, 2014.
94. Heh, D. Y. and E. L. Tan, "Divergence-preserving alternating direction implicit scheme for multi-pole Debye dispersive media," *IEEE Microw. Wireless Compon. Lett.*, Vol. 24, No. 2, 69–71, 2014.
95. Ahmed, I, E. K. Chua, E. P. Li, and Z. Chen, "Development of the three-dimensional unconditionally stable LOD-FDTD method," *IEEE Trans. Antennas Propag.*, Vol. 56, No. 11, 3596–3600, 2008.
96. Saxena, A. K. and K. V. Srivastava, "A three-dimensional unconditionally stable five-step LOD-FDTD method," *IEEE Trans. Antennas Propag.*, Vol. 62, No. 3, 1321–1329, 2014.
97. Yang, Z., E. L. Tan, and D. Y. Heh, "Second-order temporal-accurate scheme for 3-D LOD-FDTD method with three split matrices," *IEEE Antennas Wireless Propag. Lett.*, Vol. 14, 1105–1108, 2015.
98. Yang, Z., E. L. Tan, and D. Y. Heh, "Variants of second-order temporal-accurate 3-D FLOD-FDTD schemes with three split matrices," *IEEE Int. Conf. Comput. Electromagn.*, 265–267, Guangzhou, 2016.
99. Tan, E. L. and D. Y. Heh, "M1-D FDTD methods for mobile interactive teaching and learning of wave propagation in transmission lines," *IEEE Antennas Propag. Mag.*, Vol. 61, No. 5, 119–126, 2019.
100. Yang, Z. and E. L. Tan, "Interconnected multi-1-D FADI- and FLOD-FDTD methods for transmission lines with interjunctions," *IEEE Trans. Microw. Theory Tech.*, Vol. 65, No. 3, 684–692, 2017.
101. Tan, E. L. and D. Y. Heh, "Demonstration of electromagnetic waves propagation along transmission lines on iPad," *2018 Joint IEEE Int. Symp. Electromag. Compat. and Asia-Pacific*

Symp. Electromag. Compat., 599–601, Singapore, 2018.

102. Yang, Z. and E. L. Tan, "Non-uniform time-step FLOD-FDTD method for multiconductor transmission lines including lumped elements," *IEEE Trans. Electromagn. Compat.*, Vol. 59, No. 6, 1983–1992, 2017.
103. Yang, Z. and E. L. Tan, "Multiple one-dimensional FDTD method for coupled transmission lines and stability condition," *IEEE Microw. Wireless Compon. Lett.*, Vol. 26, No. 11, 864–866, 2016.
104. Yang, Z. and E. L. Tan, "Multiple one-dimensional finite-difference time-domain method for asymmetric coupled transmission lines," *IEEE Int. Conf. Comput. Electromagn.*, Chengdu, 2018.
105. Paul, C. R., *Analysis of Multiconductor Transmission Lines*, 2nd edition, Wiley, New York, 2008.
106. Mongia, R. K., I. J. Bahl, P. Bhartia, and J. Hong, *RF and Microwave Coupled-line Circuits*, 2nd edition, Artech House, Norwood, MA, USA, 2007.
107. Pozar, D. M., *Microwave Engineering*, 4th edition, Wiley, New York, 2011.
108. Heh, D. Y. and E. L. Tan, "Unconditionally stable multiple one-dimensional ADI-FDTD method for coupled transmission lines," *IEEE Trans. Antennas Propag.*, Vol. 66, No. 12, 7488–7492, 2018.
109. Heh, D. Y. and E. L. Tan, "Numerical stability analysis of M1-D ADI-FDTD method for coupled transmission lines," *IEEE Int. Conf. Comput. Electromagn.*, Shanghai, 2019.
110. Tan, E. L. and D. Y. Heh, "Source-incorporated M1-D FADI-FDTD method for coupled transmission lines," *11th Int. Conf. Microw. Millimeter Wave Techn.*, Guangzhou, 2019.
111. Tan, E. L. and D. Y. Heh, "Multiple 1-D fundamental ADI-FDTD method for coupled transmission lines on mobile devices," *IEEE J. Multiscale Multiphys. Comput. Tech.*, Vol. 4, 198–206, 2019.
112. Tan, E. L. and D. Y. Heh, "Mobile teaching and learning of coupled-line structures," *IEEE Antennas Propag. Mag.*, Vol. 62, No. 4, 62–69, 2020.
113. Heh, D. Y. and E. L. Tan, "Numerical stability analysis of M1-D LOD-FDTD method for inhomogeneous coupled transmission lines," *IEEE AP-S Int. Symp. Antennas Propag.*, 1657–1658, Atlanta, 2019.
114. Heh, D. Y. and E. L. Tan, "Multiple LOD-FDTD method for inhomogeneous coupled transmission lines and stability analyses," *IEEE Trans. Antennas Propag.*, Vol. 68, No. 3, 2198–2205, 2020.
115. Tan, E. L. and S. Y. Tan, "Spectral-domain dyadic Green's functions for surface current excitation in planar stratified bianisotropic media," *IEE Proc. Microw. Antennas Propag.*, Vol. 146, No. 6, 394–400, 1999.
116. Tan, E. L. and S. Y. Tan, "Unbounded and scattered field representations of the dyadic Green's functions for planar stratified bianisotropic media," *IEEE Trans. Antennas Propag.*, Vol. 49, No. 8, 1218–1225, 2001.
117. Tan, E. L., "Note on formulation of the enhanced scattering- (transmittance-) matrix approach," *J. Opt. Soc. Am. A*, Vol. 19, No. 6, 1157–1161, 2002.
118. Tan, E. L., "Recursive asymptotic impedance matrix method for electromagnetic waves in bianisotropic media," *IEEE Microw. Wireless Compon. Lett.*, Vol. 16, No. 6, 351–353, 2006.
119. Ning, J. and E. L. Tan, "Hybrid matrix method for stable analysis of electromagnetic waves in stratified bianisotropic media," *IEEE Microw. Wireless Compon. Lett.*, Vol. 18, No. 10, 653–655, 2008.
120. Ning, J. and E. L. Tan, "Generalized eigenproblem of hybrid matrix method for stable analysis of periodic multilayered bianisotropic media," *Asia-Pacific Microwave Conf.*, Hong Kong, 2008.
121. Tan, E. L. and S. Y. Tan, "Singularities and discontinuities in the eigenfunction expansions of the dyadic Green's functions for biisotropic media," *Progress In Electromagnetics Research*, Vol. 19, 301–318, 1998.
122. Tan, E. L. and S. Y. Tan, "A unified representation of the dyadic Green's functions for planar, cylindrical and spherical multilayered biisotropic media," *Progress In Electromagnetics Research*, Vol. 20, 75–100, 1998.
123. Tan, E. L. and S. Y. Tan, "Dyadic Green's functions for circular waveguides filled with biisotropic media," *IEEE Trans. Microw. Theory Tech.*, Vol. 47, No. 7, 1134–1137, 1999.

124. Tan, E. L., "Unified solutions of static Green's functions for open and covered planar two-layered anisotropic media," *IEEE AP-S Int. Symp. Antennas Propag.*, 892–895, Salt Lake City, 2000.
125. Tan, E. L., "Electrostatic Green's functions for planar multilayered anisotropic media," *IEE Proc. Microw. Antennas Propag.*, Vol. 149, No. 1, 78–83, 2002.
126. Ning, J. and E. L. Tan, "Simple and stable analysis of multilayered anisotropic materials for design of absorbers and shields," *Mater. Des.*, Vol. 30, No. 6, 2061–2066, 2009.
127. Tan, E. L. and S. Y. Tan, "Cylindrical vector wave function representations of electromagnetic fields in gyrotropic bianisotropic media," *Journal of Electromagnetic Waves and Applications*, Vol. 13, No. 11, 1461–1476, 1999.
128. Tan, E. L. and S. Y. Tan, "Cylindrical vector wave function representations of the dyadic Green's functions for cylindrical multilayered gyrotropic bianisotropic media," *Progress In Electromagnetics Research*, Vol. 26, 199–222, 2000.
129. Tan, E. L. and S. Y. Tan, "On the eigenfunction expansions of the dyadic Green's functions for bianisotropic media," *Progress In Electromagnetics Research*, Vol. 20, 227–247, 1998.
130. Tan, E. L. and S. Y. Tan, "Coordinate-independent dyadic formulation of the dispersion relation for bianisotropic media," *IEEE Trans. Antennas Propag.*, Vol. 47, No. 12, 1820–1824, 1999.
131. Tan, E. L. and S. Y. Tan, "Concise spectral formalism in the electromagnetics of bianisotropic media," *Progress In Electromagnetics Research*, Vol. 25, 309–331, 2000.
132. Tan, E. L., "Vector wave function expansions of dyadic Green's functions for bianisotropic media," *IEE Proc. Microw. Antennas Propag.*, Vol. 149, No. 1, 57–63, 2002.
133. Tan, E. L., "Reduced conditions for the constitutive parameters of lossy bi-anisotropic media," *Microwave Opt. Technol. Lett.*, Vol. 41, No. 2, 133–135, 2004.
134. Tan, E. L., "Enhanced R-matrix algorithms for multilayered diffraction gratings," *Appl. Opt.*, Vol. 45, No. 20, 4803–4809, 2006.
135. Tan, E. L., "Hybrid-matrix algorithm for rigorous coupled-wave analysis of multilayered diffraction gratings," *J. Mod. Opt.*, Vol. 53, No. 4, 417–428, 2006.
136. Ning, J. and E. L. Tan, "Generalized eigenproblem of hybrid matrix for Bloch-Floquet waves in one-dimensional photonic crystals," *J. Opt. Soc. Am. B*, Vol. 26, No. 4, 676–683, 2009.
137. Tan, E. L. and Y. W. M. Chia, "Green's function and network analysis of quasi-2D SAW ID-tags," *IEEE Ultrasonics Symp.*, 55–58, San Juan, Puerto Rico, 2000.
138. Tan, E. L., "A robust formulation of SAW Green's functions for arbitrarily thick multilayers at high frequencies," *IEEE Trans. Ultrason., Ferroelec., Freq. Contr.*, Vol. 49, No. 7, 929–936, 2002.
139. Tan, E. L., "A concise and efficient scattering matrix formalism for stable analysis of elastic wave propagation in multilayered anisotropic solids," *Ultrasonics*, Vol. 41, No. 3, 229–236, 2003.
140. Tan, E. L., "Stiffness matrix method with improved efficiency for elastic wave propagation in layered anisotropic media," *J. Acoust. Soc. Am.*, Vol. 118, No. 6, 3400–3403, 2005.
141. Tan, E. L., "Hybrid compliance-stiffness matrix method for stable analysis of elastic wave propagation in multilayered anisotropic media," *J. Acoust. Soc. Am.*, Vol. 119, No. 1, 45–53, 2006.
142. Tan, E. L., "Generalized eigenproblem for acoustic wave propagation in periodically layered anisotropic media," *J. Comput. Acoustics*, Vol. 16, No. 1, 1–10, 2008.
143. Tan, E. L., "Generalized eigenproblem of hybrid matrix for Floquet wave propagation in one-dimensional phononic crystals with solids and fluids," *Ultrasonics*, Vol. 50, No. 1, 91–98, 2010.
144. Tan, E. L., "Recursive asymptotic hybrid matrix method for acoustic waves in multilayered piezoelectric media," *Open J. Acoustics*, Vol. 1, 27–33, 2011.
145. Tan, E. L., "Simple derivation and proof of geometrical stability criteria for linear two-ports," *Microwave Opt. Technol. Lett.*, Vol. 40, No. 1, 81–83, 2004.
146. Tan, E. L., "Simplified graphical analysis of linear three-port stability," *IEE Proc. Microw. Antennas Propag.*, Vol. 152, No. 4, 209–213, 2005.
147. Tan, E. L., J. Ning, and K. S. Ang, "Geometrical stability criteria for two-port networks in invariant immittance parameters representation," *Asia-Pacific Microwave Conf.*, Hong Kong, 2008.

148. Tan, E. L., "Comments on 'Distance from unconditional stability boundary of a two-port network'," *IET Microw. Antennas Propag.*, Vol. 8, No. 1, 64, 2014.
149. Tan, E. L., "Rollett-based single-parameter criteria for unconditional stability of linear two-ports," *IEE Proc. Microw. Antennas Propag.*, Vol. 151, No. 4, 299–302, 2004.
150. Tan, E. L., X. Sun, and K. S. Ang, "Unconditional stability criteria for microwave networks," *Progress In Electromagnetics Research Symposium*, 1524–1528, Beijing, China, March 23–27, 2009.
151. Tan, E. L., "A Quasi-invariant single-parameter criterion for linear two-port unconditional stability," *IEEE Microw. Wireless Compon. Lett.*, Vol. 14, No. 10, 487–489, 2004.
152. Tan, E. L., "Quasi-invariant single-parameter criterion for unconditional stability: Review and application," *Asia-Pacific Microwave Conf.*, 429–432, Yokohama, 2006.
153. Tan, E. L. and S. Z. Fan, "Graphical analysis of stabilization loss and gains for three-port networks," *IEEE Trans. Microw. Theory Tech.*, Vol. 60, No. 6, 1635–1640, 2012.
154. Tan, E. L. and D. Y. Heh, "Application of Belevitch theorem for pole-zero analysis of microwave filters with transmission lines and lumped elements," *IEEE Trans. Microw. Theory Tech.*, Vol. 66, No. 11, 4669–4676, 2018.
155. Tan, E. L. and D. Y. Heh, "Analysis and determination of microwave filter order," *Asia-Pacific Microwave Conf.*, 1360–1362, Kyoto, 2018.
156. Tan, E. L. and D. Y. Heh, "Pole-zero analysis of microwave filters using contour integration method exploiting right-half plane," *Progress In Electromagnetics Research M*, Vol. 78, 59–68, 2019.
157. Smunyahirun, R. and E. L. Tan, "Derivation of the most energy-efficient source functions by using calculus of variations," *IEEE Trans. Circuits Syst. I: Regul. Pap.*, Vol. 63, No. 4, 494–502, 2016.
158. Smunyahirun, R. and E. L. Tan, "Optimum lowest input energy for first-order circuits in transient state," *Int. Conf. Electrical Engineering/Electronics, Computer, Telecommunications and Information Technology*, 143–146, Phuket, 2017.
159. Smunyahirun, R. and E. L. Tan, "Most energy-efficient input voltage function for RC delay line," *2018 Joint IEEE Int. Symp. Electromag. Compat. and Asia-Pacific Symp. Electromag. Compat.*, 1022–1026, Singapore, 2018.